

# Effects of frontal processes on marine aggregate dynamics and fluxes: An interannual study in a permanent geostrophic front (NW Mediterranean)

Lars Stemmann<sup>a,b,\*</sup>, Louis Prieur<sup>a,b</sup>, Louis Legendre<sup>a,b</sup>, Isabelle Taupier-Letage<sup>c</sup>,  
Marc Picheral<sup>a,b</sup>, Lionel Guidi<sup>a,b</sup>, Gabriel Gorsky<sup>a,b</sup>

<sup>a</sup> CNRS, Laboratoire d'Océanographie de Villefranche, BP 28, 06234 Villefranche-sur-Mer CEDEX, France

<sup>b</sup> Université Pierre et Marie Curie-Paris6, LOV, Villefranche-sur-Mer, France

<sup>c</sup> Laboratoire d'Océanographie et de Biogéochimie (LOB), CNRS UMR 6535, Université de la Méditerranée, Centre d'Océanologie de Marseille, Antenne de Toulon, c/o IFREMER, BP 330, 83507 La Seyne Cedex, France

Received 15 December 2005; received in revised form 31 January 2007; accepted 2 February 2007

Available online 16 February 2007

## Abstract

This study provides and discusses the spatial distributions of abundances and sizes of marine-snow aggregates across the Ligurian Sea frontal system. A cross-front transect was sampled 34 times between 1992 and 1996, using the Underwater Video Profiler (UVP). Atlantic Water flows parallel to the Ligurian coast in the NW Mediterranean Sea, where that current creates a quasi-permanent front that separates the central and coastal waters. The horizontal distribution of aggregates ( $> 150 \mu\text{m}$  ESD, Equivalent Spherical Diameter) in the upper 1000 m shows two main features. First, the smaller aggregates ( $150 \mu\text{m} < \text{ESD} < 1 \text{ mm}$ ) are more abundant in coastal waters, as a result of continental input, cross-slope export, and re-suspension along the slope. The layers that contain very high concentrations of small aggregates are observed from surface down to 1000 m, and extend from the continental slope to the front. Second, the concentrations of large aggregates ( $\text{ESD} > 1 \text{ mm}$ ) are highest in and under the frontal zone, probably as a result of physical coagulation, and/or biological transformations. The seasonal intensity of large aggregate accumulations in and under the frontal structure seems to be more related to the autumn–winter increase in sub-mesoscale and mesoscale activity of the current flow than to the surface phytoplankton biomass. Interestingly, the horizontal distribution of aggregates is affected not only in the frontal zone (0–300 m depth), but also deeper down to 1000 m, probably as a consequence of rapid sinking or vertical transport. Results suggest that the settling of large aggregates under the frontal zone may limit the cross-slope transport of fine-grained particles by coagulation due to differential settling between the small particles suspended in the continental nepheloid layer and the large aggregates. This process, which takes place in sub-mesoscale zones (5–10 km wide), was also observed in one other front in the Western Mediterranean Sea. This led us to hypothesize that the impact of frontal processes on particle and aggregate dynamics might be generalized. Since fronts exist in many other coastal regions, the vertical fluxes at sub-mesoscale may have consequences for the transport of continental particles to the ocean's interior.

© 2007 Elsevier B.V. All rights reserved.

**Keywords:** Marine-snow; Aggregates; Plankton; Vertical flux; Fronts; Mesoscale features; Mediterranean Sea

\* Corresponding author. CNRS, Laboratoire d'Océanographie de Villefranche, BP 28, 06234 Villefranche-sur-Mer CEDEX, France.  
E-mail address: [stemmann@obs-vlr.fr](mailto:stemmann@obs-vlr.fr) (L. Stemmann).

## 1. Introduction

In the last 20 years, there have been several large programs on shelf-edge exchange processes, designed to quantify the role of continental shelves and slopes as sinks for atmospheric CO<sub>2</sub>. Intermediate Nepheloid Layers (INLs) off the continental slopes were observed at several sites (Gardner, 1989; de Madron et al., 1999a; Heussner et al., 1999; McCave et al., 2001). Authors have invoked various biological, physical, or combined mechanisms related to marine aggregates to explain the dynamics of INLs (Gardner and Walsh, 1990; Monaco et al., 1990; McCave et al., 2001). It was proposed that large marine aggregates, which include various types of particles (biogenic and mineral), are major players in the aggregation of fine suspended particles and their subsequent horizontal or vertical transport. At the Gulf of Lions shelf edge, just to the west of the present study area, Durrieu de Madron et al. (1990) proposed that the spatial extent of the INLs was controlled by the presence of a permanent frontal structure generated by the permanent along-slope current of the Atlantic Water (AW). In addition, Monaco et al. (1990) suggested that the offshore spreading of the INL was controlled by the scavenging of small particles by large settling aggregates produced above, in the euphotic zone. However, the spatial scale at which the scavenging of INLs by large aggregates occurs is not known.

A recent study, conducted in the mesoscale context of the North-East Atlantic, has shown that the abundance of

large aggregates increases as deep as 1000 m depth, probably resulting from intense mesoscale export of surface production (Guidi et al., 2007). In addition, another recent study across the Almeria frontal systems, along the continental slope of the Algerian coast, suggested that aggregates larger than 1 mm ESD (Equivalent Spherical Diameter) were more abundant in the vicinity of the front than in adjacent waters (Gorsky et al., 2002). The authors proposed that the accumulation of large aggregates close to the front may increase the deep vertical transport of particles at horizontal scales of few tens of kilometers. Therefore, it is possible that such local export at fronts along the continental slope could potentially sweep the suspended particles contained in the INLs. However, the spatial and temporal distributions of aggregates at shelf edges are still poorly known, especially in mesoscale features.

The objectives of the present work are to provide estimates of the spatial variability in the vertical distributions of aggregates (60–1000 m) across the Ligurian Sea frontal system (Fig. 1), in order to test the hypotheses that (1) the offshore spreading of coastal suspended particles and aggregates is controlled by the frontal structure, (2) the offshore extension of INLs is controlled by higher vertical export of large aggregates under the frontal zone. Results from our study will be compared with an investigation made in the Almeria frontal system. Similarity in patterns of variability would provide a basis for defining the spatial distribution of

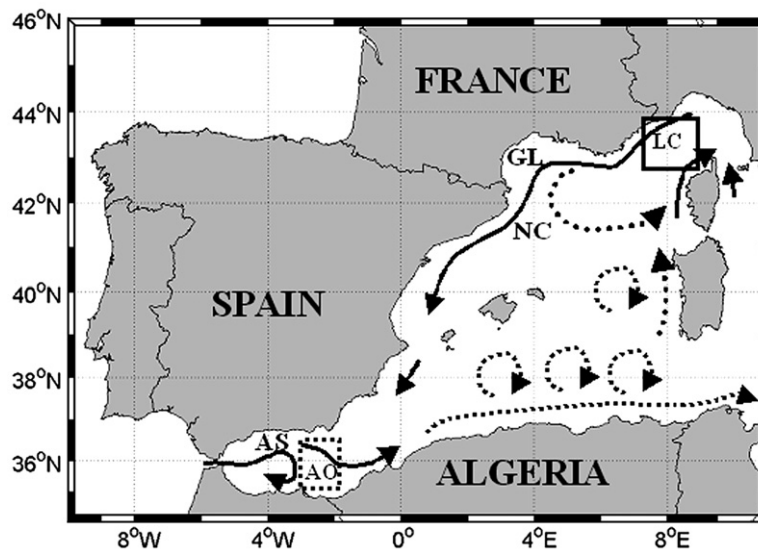


Fig. 1. Sampling zones in the Western Mediterranean Sea (LC=Ligurian Current, NC=Northern Current, AS=Alboran Sea, GL=Gulf of Lion). The locations of the two frontal systems are highlighted by the boxes: the Ligurian frontal system is in the upper northeastern rectangle, and the Almeria frontal system is in the southwestern rectangle. The path of the flow of the AW is represented by the continuous (more or less steady path) and dotted (mesoscale meandering throughout the year) arrows (redrawn from Millot, 1999).

aggregates in along-slope frontal systems. The occurrence of such processes along the flow of the AW in the Western Mediterranean sea will be discussed.

## 2. General features of the Ligurian Sea frontal system

The permanent cyclonic circulation in the Ligurian Sea is well documented from numerous historical (Béthoux and Prieur, 1983), hydrocast (Béthoux et al., 1988; Albérola et al., 1995), and current-meter (Taupier-Letage and Millot, 1986; Sammari et al., 1995) data. The thermal front detected from IR images corresponds to a density front which sets the offshore surface limit of the Ligurian Current (Prieur et al., 1981), and shows meanders (Crépon et al., 1982). The Ligurian Current (LC), which is about 25 km wide and 300–400 m deep, flows southwestwards along the coast, over depths greater than 1000 m, with a mean speed of 25–35 cm s<sup>-1</sup> (Béthoux et al., 1988; Albérola et al., 1995; Sammari et al., 1995; Millot, 1999). It is a component of the Northern Mediterranean Current,

which transports light Atlantic Water from Italy towards Spain (Prieur et al., 1983; Millot, 1999). Béthoux et al. (1982) showed that transport in the upper 200 m (annual mean ca. 1.4 Sv) has a marked seasonal variability due to the permanent contribution of the Western Corsica Current (0.7 Sv) and a seasonal contribution of flow from the Tyrrhenean Sea through the Corsica Channel (from 2 Sv in late autumn to a minimum of 0.2 Sv in summer). Later measurements in the Corsica Channel confirmed this seasonal variation and stressed the inter-annual variability in intensity and periodicity which is associated with the heat and water losses in Ligurian Sea (Astraldi and Gasparini, 1992).

Dense water is formed in the Central Zone (CZ) of the Ligurian Sea as a consequence of meteorological forcing in winter. Subsequent geostrophic adjustment accelerates the LC flow in winter around the CZ (Crépon and Boukthir, 1987). Out of the winter period, the LC flow is also forced by two other processes, i.e. the discharge of freshwater along the coast following heavy rains in autumn and, from spring to next winter, the 100 m

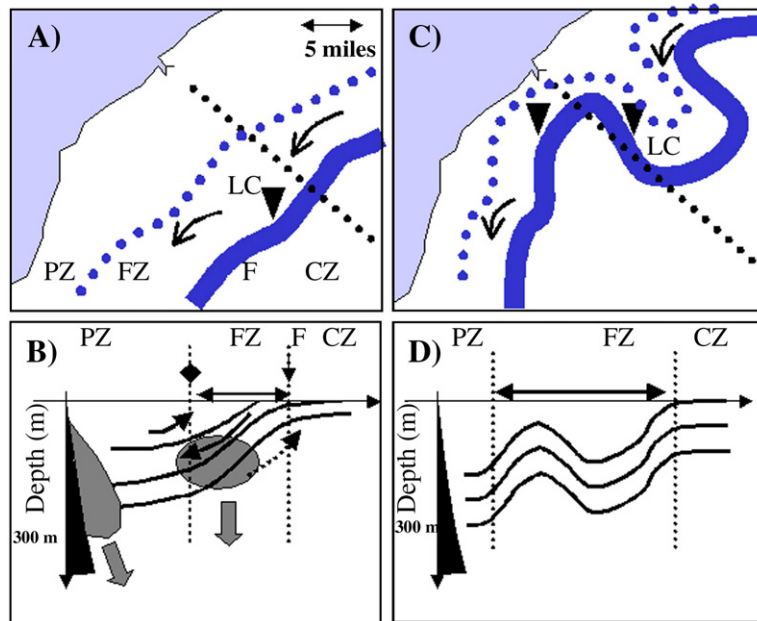


Fig. 2. Schematic representation of the position of the sampled transect relative to the Ligurian Current (LC) in two extremes situation. A and C are horizontal maps and the grey area corresponds to land, B and D are vertical sections and the black triangle represents the continental slope. A and B depict the summer situation, with a broad current and low mesoscale activity, C and D are the winter situation, with a narrow current and a sharp meander such as in February 1996. In A and C, the dotted straight line is the transect, the thick continuous curve is the front, the dotted curve is the coastal limit of the current, the black triangles symbolize the main processes associated to these situations, as follows: (▼) convergence, downwelling, and (▲) divergence, upwelling. The arrows (↖) in A and C indicate the mean flow of the horizontal current. The double arrow in A represents 5 miles, and the front in A is located at approximately 20 miles from the coast. In B and D, the symbols ◆ and ↓ indicate the coastal and offshore limits of the frontal zone (FZ), respectively. The FZ separates the Peripheral Zone (PZ) from the Central Zone (CZ). The arrows in B represent the main processes associated with this situation: (↖) convergence and downwelling, and (↗) divergence and upwelling (the same arrows are found in Boucher et al., 1987). In B, the gray area along the slope corresponds to INL and IAL, of continental and biogenic origin, while the gray area in the FZ corresponds to IAL locally produced and being exported vertically below the front section (see Discussion).

lowering of the dense water level in the CZ due to outflow of dense water at Gibraltar (Béthoux et al., 1988). Under the influence of these forcings and also winds, the LC is subject to frontogenetic processes and geostrophic adjustments, which generate meandering, and secondary circulation with possible strong, local vertical velocities near the front. This mesoscale activity is highest from early autumn to late winter (Sammari et al., 1995). Therefore the LC is not a coastal current but an along-slope current with high horizontal velocity in the jet and weak velocity near the coast ( $5 \text{ cm s}^{-1}$  to SW). Using a quasigeostrophic approximation, Allen et al. (2005) demonstrated that, in a similar jet frontal system which was meandering and baroclinically unstable, the vertical circulation upwelled light water in the current, and downwelled near-surface dense water near the front. However, other dynamical sources of vertical circulation, such as turbulences and ageostrophic forcings, are possible and could deeply modify the vertical pattern (Giordani et al., 2006). In the Ligurian Front, as in many other studied areas, physical data are not sufficient to perform vertical velocity calculations, but the patterns in phytoplankton biomass, temperature and salinity suggest that they occur (Zakardjian and Prieur, 1998). Cooler water, richer in nutrients, is often encountered along the front at surface, which is consistent with upwelling of subsurface water (Boucher et al., 1987; Sournia et al., 1990). In addition, double-peaked chlorophyll and nitrate vertical profiles are frequently observed near the offshore side of the LC (Boucher et al., 1987). The deep peaks in the frontal zone are the signatures of convergence and downward advection along isopycnals of the production in the CZ. Such anomalies are not necessarily due to continuous vertical circulation, but could be also modulated by marginal instabilities of the jet when it is strongly meandering. This geostrophic frontal system has a strong impact year long on the upper distributions of phytoplankton and zooplankton in the Ligurian Sea (Boucher et al., 1987; Sournia et al., 1990; Goffart et al., 1995). Furthermore, lateral export of surface production along isopycnals in the convergence has been proposed to feed the observed mesopelagic appendicularian communities in the mesopelagic coastal zone (Gorsky et al., 1991).

In a schematic model, Boucher et al. (1987) assumed divergence near the offshore limits of the current jet, and convergence inside the frontal zone. The same physical scheme is used in the present work (Fig. 2). As the LC is a geostrophic frontal jet, with its core flowing roughly above the 1500–2000 m isobath (15 nautical miles off Nice), vertical sections of density allow the delimitation of the jet and the front. It is difficult to determine precisely the coastal limit of the jet from density sections only, but

Table 1  
Position of the stations in the Ligurian Sea

Station	Latitude	Longitude	Distance (nm)
13	43°39.58	07°21.39	1.5
12	43°38.73	07°23.08	3
10bis	43°37.90	07°24.93	4.5
10	43°37.72	07°25.85	5.5
9	43°36.07	07°28.99	8
8	43°34.69	07°31.88	10.5
7	43°33.36	07°34.78	13
6	43°32.00	07°37.68	15.5
5	43°30.67	07°40.57	18
4	43°29.28	07°43.39	20.5
3	43°27.93	07°46.39	23
2	43°26.69	07°49.25	25.5
1	43°25.29	07°52.13	28

Distance refers to the distance from Cap Ferrat on the coast open sea transect.

that limit can be determined from dynamic heights when the maximum depth of each cast is sufficiently deep (700 m in the Ligurian Sea). The frontal jet current clearly separates the peripheral zone near the coast (PZ), which contains the less saline and warmer AW, from more saline and colder water in the CZ. In the present study, the area showing a horizontal density gradient over a significant vertical scale will be identified as the Frontal Zone (FZ), and its open sea limit will be set where the seaward surface density gradient becomes considerably reduced (Fig. 2). The FZ encompasses the horizontal flow of AW as well as the convergence, whereas the CZ is characterized by weaker horizontal flow and marks the beginning of the divergence. The well studied current circulation and biological pattern in the zone provided an ideal case for examining the relation between physical forcing and marine aggregates spatial distributions.

### 3. Methods

#### 3.1. Sampling strategy

The Meso-Bathy-Pelagic Front program was conducted from January 1992 to June 1996 along a transect that crossed the typical hydrological features of the Ligurian Sea (Fig. 2). The stations were spaced every 2.5 miles (4.64 km) on the transect, from a coastal station 1.5 miles from Cap Ferrat, France, to an offshore station 28 miles (52 km) to the southeast (Table 1). Several stations were occupied in each hydrological structure (PZ, FZ and CZ, Fig. 2). A typical cruise consisted of 10–12 stations, but on one occasion data were collected at only 4 stations. The minimum time lag between two cruises was 1 day (December 1994) and the maximum was 6 months (July to December 1995 (Table 2).

Table 2

Sampling dates (first day of each cruise) during the MBP Front program (st=number of stations in the transect, \*=transect repeated within the same week)

	1992	1993	1994	1995	1996
January	13/01/92● (2 days, 10st)	27/01/93 (2 days, 11st)	12/01/94● (2 days, 12st)	15/01/95● (2 days, 11st)	
February				12/02/95● (9st)	09/02/96● (11st)
March	26/03/92 (6st)	10/03/93 (2 days, 7st)	08/03/94● (2 days, 10st)	06/03/95 (10st)	
April				03/04/95 (9st)	02/04/96 (10st)
May	26/05/92 (10st)	17/05/93 (2 days, 10st)	04/05/94● (2 days, 11st)	01/04/95 (9 st)	
June			06/06/94 (2d, 12st)		
July	07/07/92 (10st)	21/07/93 (2 days, 9st)	30/06/94 (11st)	22/07/95 (9)	
August			22/08/94 (8st)		
September	15/09/92 (2 days, 10st)	08/09/93● (2 days, 10st)			
October		05/10/93 (11st)	17/10/94 (11st, *)		
November	19/11/92 (2 days, 12st)	09/11/93● (2 days, 6 st)	24/11/94● (2 days, 7st)		
December		10/12/93 (4st)	03/12/94●● (2 days, 12 st, *)	01/12/95● (11st)	

At each station the UVP and the CTD were lowered to 1000 m, or to the bottom if shallower. ● indicates transects for which the aggregates mean size was higher in the frontal zone compared to the peripheral zone.

Defining the sampling grid to study a front is difficult because the time needed to cover the studied area overlaps with the high hydrodynamic temporal variability. In order to minimize this effect, each transect was sampled within the shortest period possible (i.e. within 0.5 to 3 days), depending on sea conditions, cruising speed of the research vessel, and the duration of the daylight period. Profiles of aggregates were recorded only during daytime, in order to avoid diurnal variations of aggregate distributions, which have been shown to influence the total particle volume in the central zone (Stemmann et al., 2000). Two tests for diel variability were conducted, one at the 8 miles station in July 1993 (8 successive profiles at 3-h intervals), and the second by repeating a day transect the following night in December 1994. The results showed no clear diurnal variability. A test for short-term variability (6 days apart) was conducted in October 1994, i.e. a period when the FZ is wide and the current reduced; it showed only small variability. These results validate the use of profiles recorded several days apart. Finally, several of the transects selected for detailed analyses were recorded within the same day.

At each station, hydrographic measurements were conducted with a Seabird CTD SBE19 from surface to 1000 m (only 300 m from January 1992 to January

1993). A Seatech fluorometer was added to the water sensor package at the beginning of 1993. In December 1994, a Seabird CTD 911 equipped with a transmissiometer was used. The time series of local rivers runoff (Var) were obtained at the 'Direction Départementale de l'Environnement', and were used to assess the correlation between aggregates and continental inputs by rivers.

### 3.2. Underwater Video Profiler

The Underwater Video Profiler (UVP) monitors the abundances, sizes and shapes of objects at a rate of 25 Hz from surface down to 1000 m (Gorsky et al., 1992). For the quantitative study of particles, the camera records objects illuminated in a 1.5 cm thick volume of water (0.28 l). With a lowering speed of  $1 \text{ m s}^{-1}$ , frames are recorded every 4 cm so that successive images do not overlap. The recorded images are digitized and automatically treated by an image analysis software. Calibration experiments in a seawater tank, using known particles of two types, i.e. dense marine aggregates (fecal pellets, copepods molts) and transparent aggregates (mucous particles, gelatinous zooplankton) showed that the UVP detects particles  $> 100 \mu\text{m}$  ESD and that a single relation can be used for all types of particle. The metric surface ( $Y$ , measured

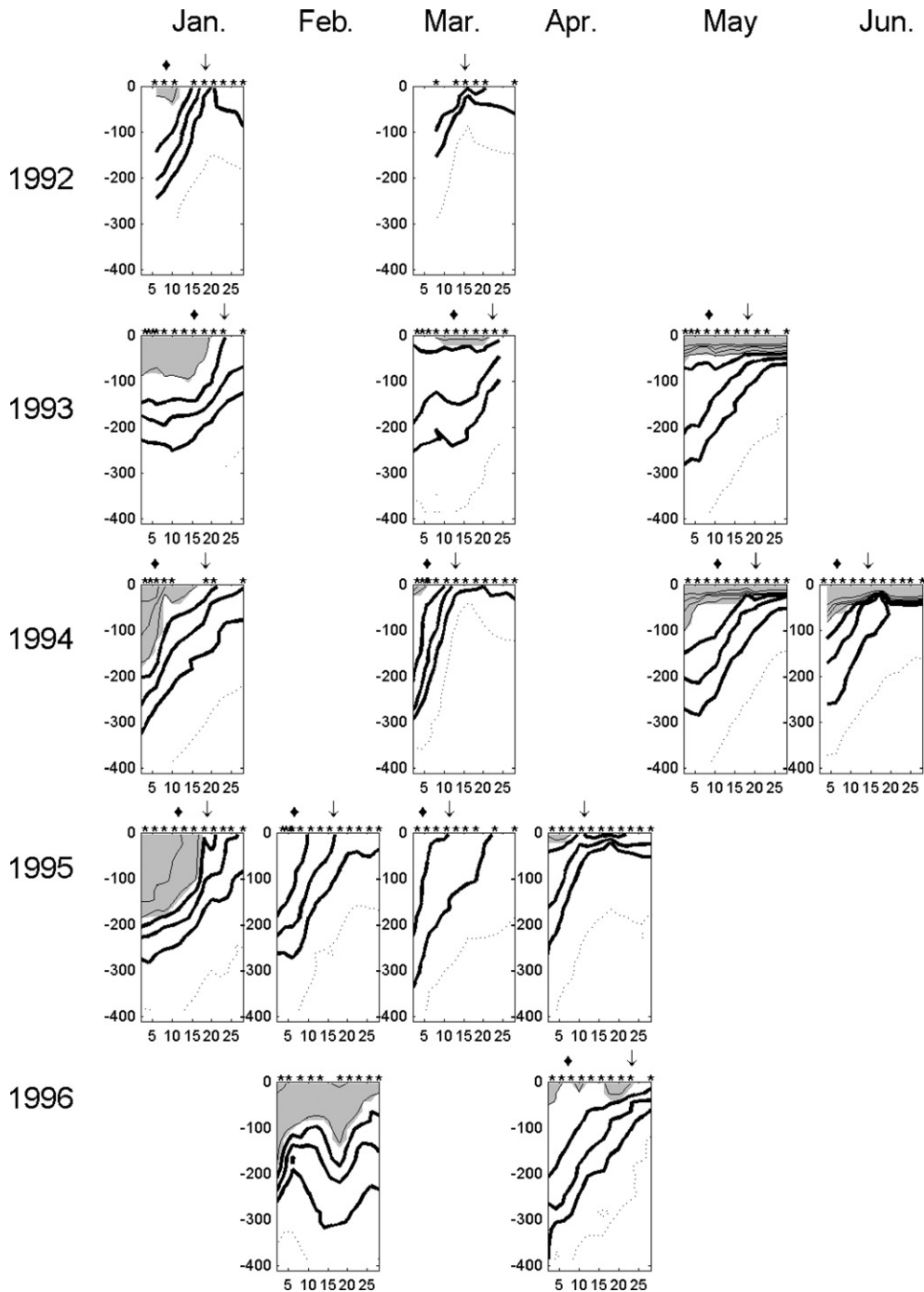


Fig. 3. Density sections from January to June. The horizontal axis is the distance from the shore in miles, and the vertical axis is depth (0–400 m). The isopycnals are identical on all panels so as to highlight seasonal variability. The 28.85, 28.95 and 29.05 isopycnals are highlighted because this density band can be considered as the interface between light and dense waters. The gray area corresponds to the zone where the density is lower than 28.65. The stars indicate the positions of the stations (with a vertical resolution of 5 m). The symbols  $\blacklozenge$  and  $\downarrow$  indicate the coastal and offshore limits of the frontal zone, respectively.

under the binocular microscope) as a function of the pixel surface ( $X$ , given by the UVP image) is  $Y=0.00139 * X^{1.43}$  (Stemmann et al., 2002). This relation

was tested twice during the survey period, and no drift was observed. The area of each particle on the video profile was converted to ESD (mm). In the present

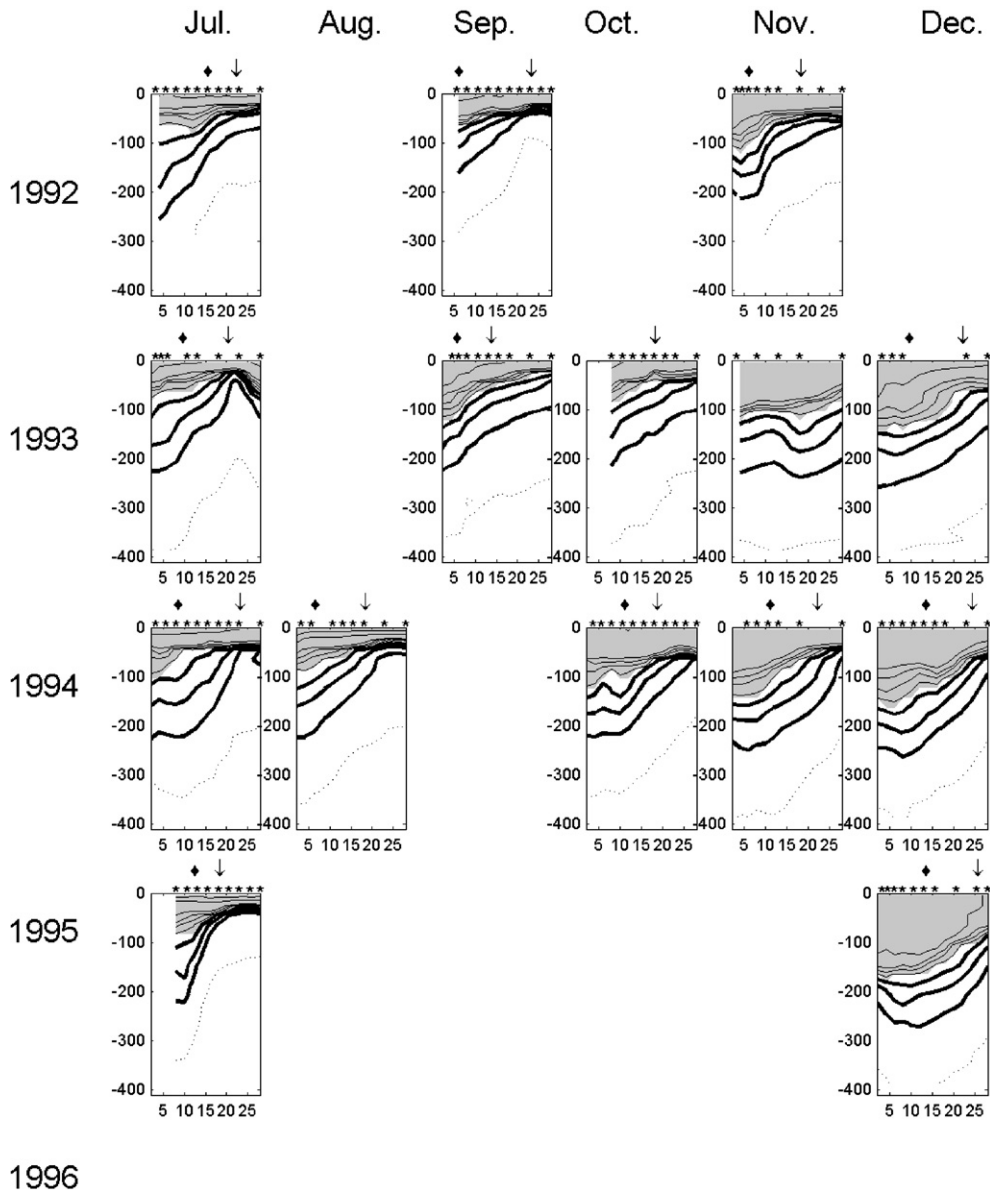


Fig. 4. Same as Fig. 3, for the months of July to December.

paper, we report vertical profiles of particles larger than 0.15 mm. We only use data from segment portions of profiles that displayed images with a dark background, because sunlight interferes with the collimated light beam. Hence, most of the data come from below 60 m, i.e. 60–1000 m.

### 3.3. Data treatment

A total of 363 UVP and CTD vertical profiles were recorded between 1992 and 1996. The CTD data were

treated using the Seabird Software (SEASOFT). The UVP images were treated with a custom-built image analysis software. Data on the vertical distribution of particles were extracted from the video images with a vertical resolution of 5 m, and a sampling volume of 7 l per depth bin (25 images every 125 images). Both data sets (CTD and UVP) were stored in a database under Matlab until further processing. Among the parameters that are available for aggregates (total abundance, total ESDVolume, median, mean or standard deviation of ESD, maximum length, whole size spectrum), we chose to

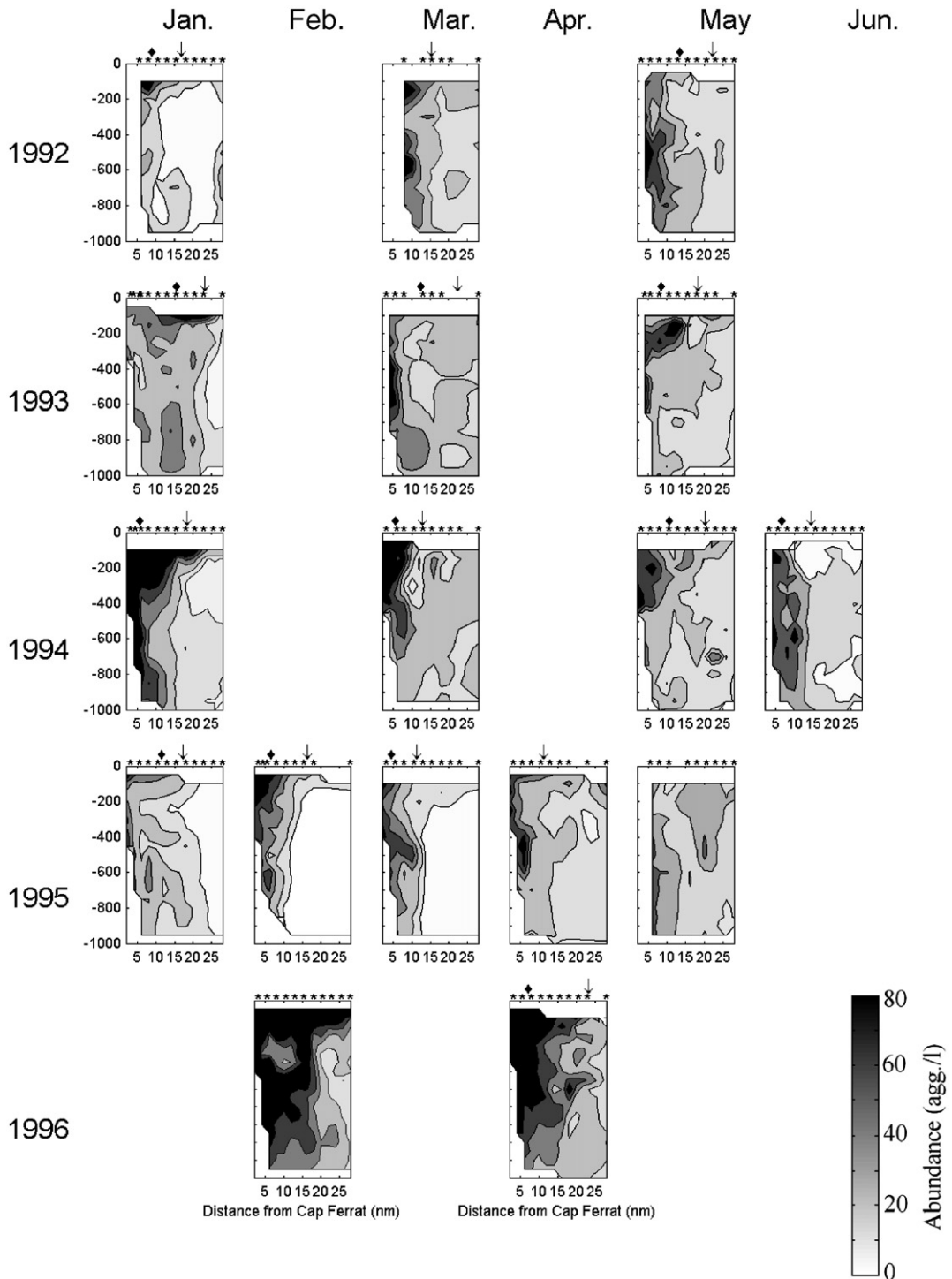


Fig. 5. Aggregate abundance (agg. l<sup>-1</sup>) distributions from January to June (1992 to 1996). The horizontal axis is the distance from the shore (one tick every 5 miles), and the vertical axis is depth (0 to 1000 m). The arrows indicate the positions of the coastal and offshore edges of the frontal zone (see Figs. 3 and 4). The white contour on the left of each section represents the continental slope. The stars indicate the positions of the stations (with a vertical resolution of 5 m). The symbols  $\blacklozenge$  and  $\downarrow$  indicate the coastal and offshore limits of the frontal zone, respectively.

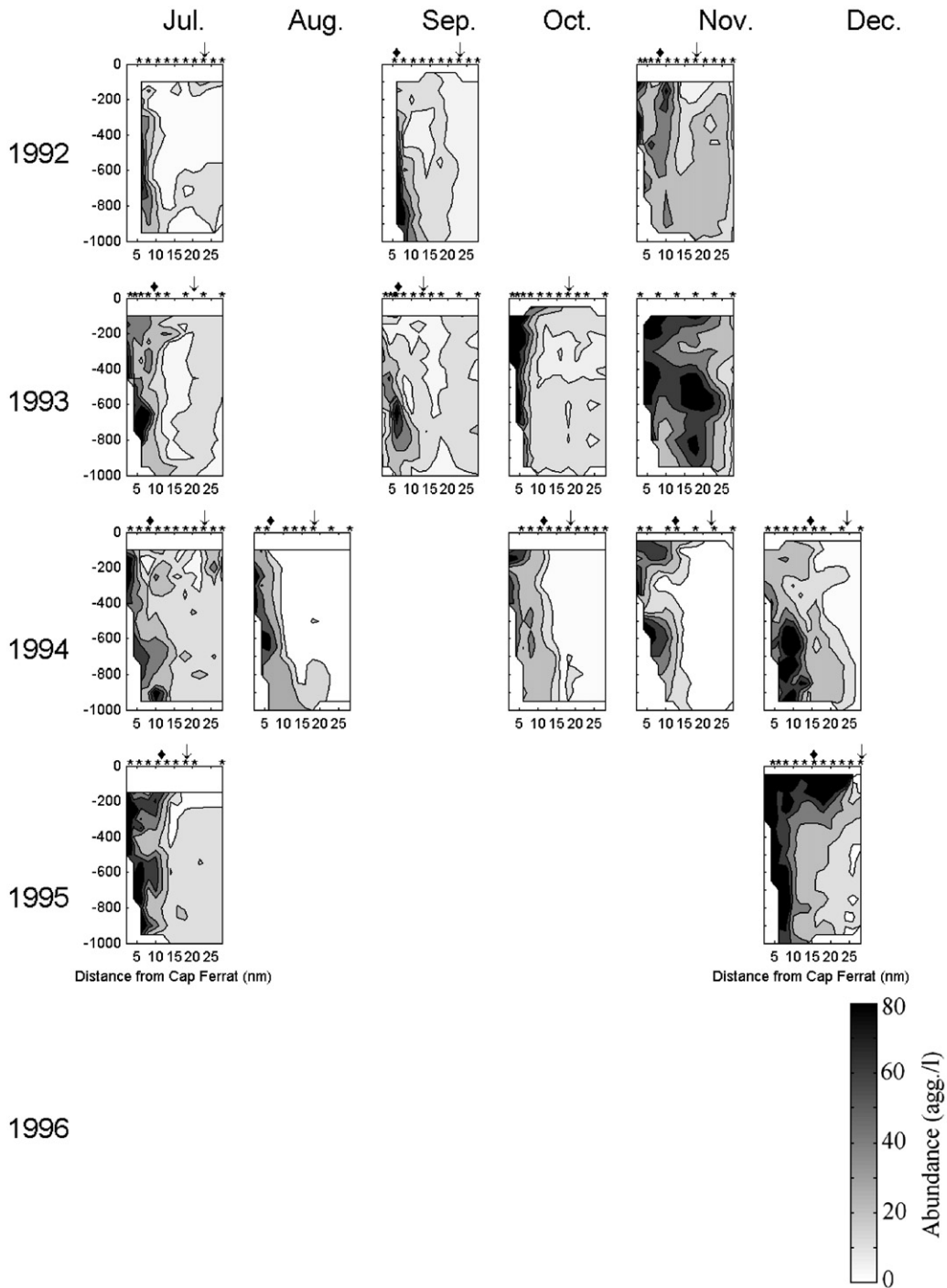


Fig. 6. Same as Fig. 5 for the months of July to December (1992–1996).

describe the aggregate populations in this work mostly by their abundances and mean ESDs. Previous studies have shown that one can derive the abundances of aggregates  $<0.5$  and  $>1$  mm from these two parameters (Stemann et al., 2002).

For the 34 UVP and 32 CTD transects, 2D sections of all variables, i.e., temperature, salinity, density, particle abundance and particle mean size, and sometimes *in situ* fluorescence and percent light transmission, were generated with Matlab (using a linear interpolation method) on a

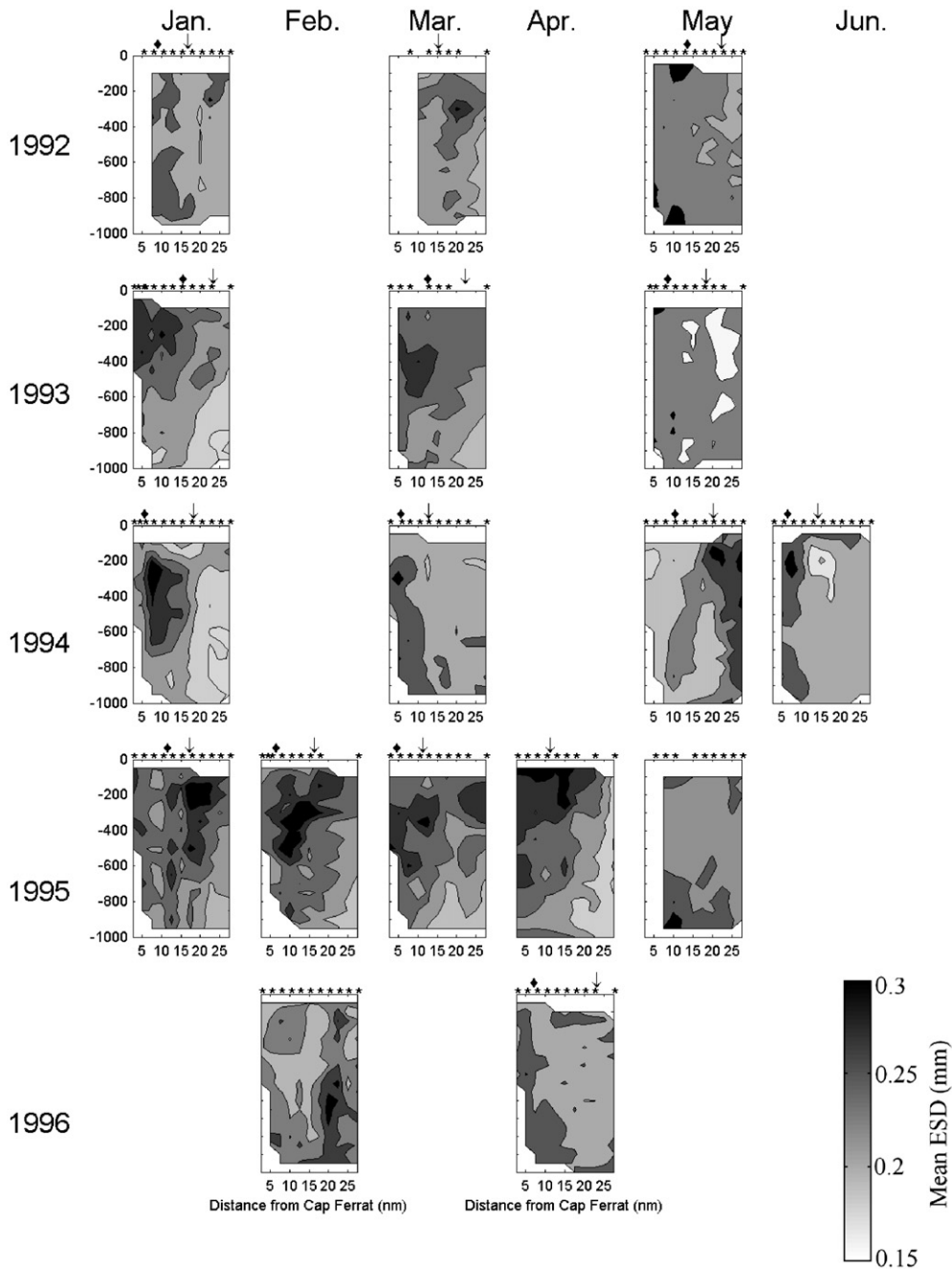


Fig. 7. Aggregate mean ESD (mm) distributions from January to June (1992 to 1996). The arrows indicate the positions of the coastal and offshore edges of the front. The horizontal axis is the distance from the shore (one tick every 5 miles), and the vertical axis is depth (0 to 1000 m). The stars indicate the positions of the stations (with a vertical resolution of 5 m). The symbols  $\blacklozenge$  and  $\downarrow$  indicate the coastal and offshore limits of the frontal zone, respectively.

vertical grid of 10 m and horizontal grid of 2.5 miles, from 5.5 to 28 miles offshore. The CTD data could not be acquired together with the UVP profiles in May 1992 and May 1995. The transect sampled in December 1993, which consisted of only 4 profiles, was removed from

further analysis. In order to test whether there were significant differences in the mean size of the aggregates in the three different zones, we divided each data set in the three subsets defined by the frontal zone limits. We re-sampled 50 data points in each subset 100 times, after

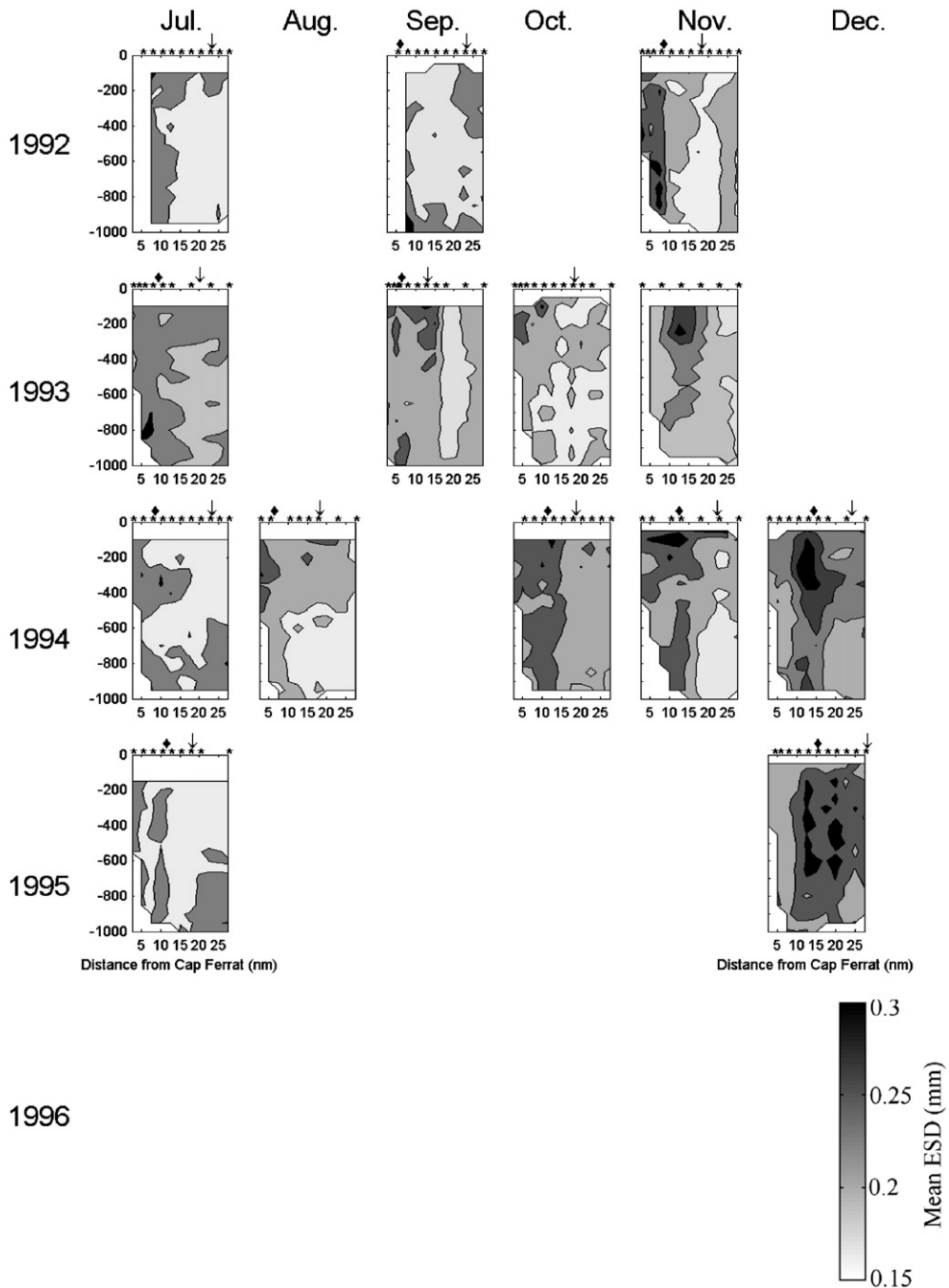


Fig. 8. Same as Fig. 7 for the months of July to December.

random permutation, and used the Kolmogorov test for two samples to assess if the differences were significant.

#### 4. Results

In most works, the terms Surface and Intermediate Nepheloid Layers stand for layers containing high load of

small micrometric particles detected by methods based on light transmission and scattering. Because the UVP detects larger particles ( $>150 \mu\text{m}$ ), we will use instead the terms Surface Aggregate Layer (SAL) and Intermediate Aggregate Layer (IAL) for aggregate-rich layers in the upper 200 m and between 200 and 1000 m depths, respectively.

#### 4.1. Density distributions

All the sections of seawater density are presented in Fig. 3 and in Fig. 4. Densities ranged between 27.55 and 29.05 kg m<sup>-3</sup>. In general, section density in the upper 200 m tended to be higher at the offshore end of transects. In this zone, the establishment of the pycnocline clearly shows summer stratification. The zones corresponding to rapid change in horizontal density correspond to the frontal zone, and the dome in isopycnals corresponds to the central water. At 5.5 miles offshore, section density at 100 m ranged between 27.55 and 28.5 kg m<sup>-3</sup> from September to December, and between 28 and 28.5 kg m<sup>-3</sup> the remainder of the year. At 28 miles, section density at 100 m, ranged between 28.95 and 29.01 kg m<sup>-3</sup> throughout the year, although some lower values were observed in January 1993, July 1993, September 1993, November 1993, December 1995, and February 1996.

In order to compare the distributions of particles to density fields, the position of the front is indicated by a vertical arrow, and the coastal limit of the FZ by a diamond symbol. In Boucher et al. (1987), the positions of the FZ were determined from continuous horizontal transects of T and S, which were not recorded in the present study. The position of the FZ on each density section was set where the slope of the density layer (28.75–28.95 kg m<sup>-3</sup>) was strong (ca 0.3 to 1%). This density band can be considered as the interface between light and dense waters<sup>1</sup>.

The frontal structure was present year round, as shown by the horizontal density gradient in the middle of the transects. The FZ separates the two main features in the North Western Ligurian Sea (i.e., PZ and CZ). In general the frontal structure is located from 13 to 23 miles offshore, but some extreme locations were observed in coastal (March 94, between 8.5 and 13 miles) and offshore (on March 93, between 15.5 and 25.5 miles) waters. The horizontal density gradients may show steps (i.e., July 1992, March 1993 and 1995, and December 1995), and sometimes decrease locally with distance from the shore (i.e., January 92, March 1992, July 1993, September 1993, and March 1994). Two major mesoscale features made it difficult to identify the front location in November 1993

and February 1996. The isopycnals slopes tended to be steeper from January to June when compared with the remainder of the year, suggesting that the LC was deeper and thinner in winter/spring. Hence, the typical frontal structure (as defined by the horizontal density gradient) was clearly detected in 28 cases out of 30, and its positions along the transect are shown in Figs. 3–8.

#### 4.2. Aggregate abundances spatial distributions

Figs. 5 and 6 show all transects for aggregate abundances from 1992 to 1996. Three out of the 34 UVP sections are not presented in Figs. 5 and 6 because there were two sets of duplicates performed within 15-day periods (October 1994, December 1994), and one section had only 4 profiles (December 1993). Aggregate concentrations ranged from 0.14 agg. l<sup>-1</sup> to 1108 agg. l<sup>-1</sup>. In general, aggregate concentrations decreased away from the coast. Typical coastal aggregate concentrations ranged from 5 to 300 agg. l<sup>-1</sup>, whereas central water aggregate concentrations ranged from 0.14 to 50 agg. l<sup>-1</sup>.

SAL and IAL contained high concentrations of aggregates (>60 agg. l<sup>-1</sup>) at all seasons along the continental slope. They never expanded offshore further than 15 miles, except in November 1993 when one IAL almost reached the offshore station (20–25 miles and 400–800 m). In all cases, the offshore limit of these layers corresponded to the position of the frontal structure (e.g. March 1994).

In January 1993, May 1993, and May 1994, high aggregate concentrations occurred in the frontal area. Seasonal variability corresponded to higher concentrations from December to May, and lower concentrations the remainder of the year. The center of the transect was particularly depleted in aggregates during summer 1994 compared to summer 1993.

#### 4.3. Aggregate mean ESD spatial distributions

Figs. 7 and 8 show the spatial distribution of mean ESD between 1992 and 1996. Values ranged from 0.2 to 0.55 mm. In general, the mean size tended to be smaller in the deepest part of the 60–1000 m water column. Highest mean ESD occurred from November to March.

There were 31 combined CTD-UVP transects, but in three cases the FZ was defined only by its offshore limit (March 92, October 93, April 1995), and three transects had less than 50 data points in one of the subsets (September 92, October 94, July 95). We analysed the remaining 25 transects with a Kolmogorov test ( $\alpha=0.01$ ). The results of the test showed that the average ESD was significantly higher in the FZ than in the PZ in 13 cases

<sup>1</sup> Using the wind thermal equation  $\partial v_g / \partial z = -(g/\rho f) \cdot \partial \rho / \partial x$ , where  $f$  is the Coriolis parameter. An along  $x$  horizontal density gradient 0.2 kg m<sup>-3</sup> over 10 km across sloping isopycnals corresponds to 20 cm s<sup>-1</sup> baroclinic geostrophic velocity if such a gradient is observed on a vertical ( $z$ ) excursion of 100 m. More precise limits of LC could not be determined systematically because numerous casts were too shallow. With such a definition, the FZ encompasses the offshore part of the LC, which is the most important for vertical circulation and its effect on biological productivity.

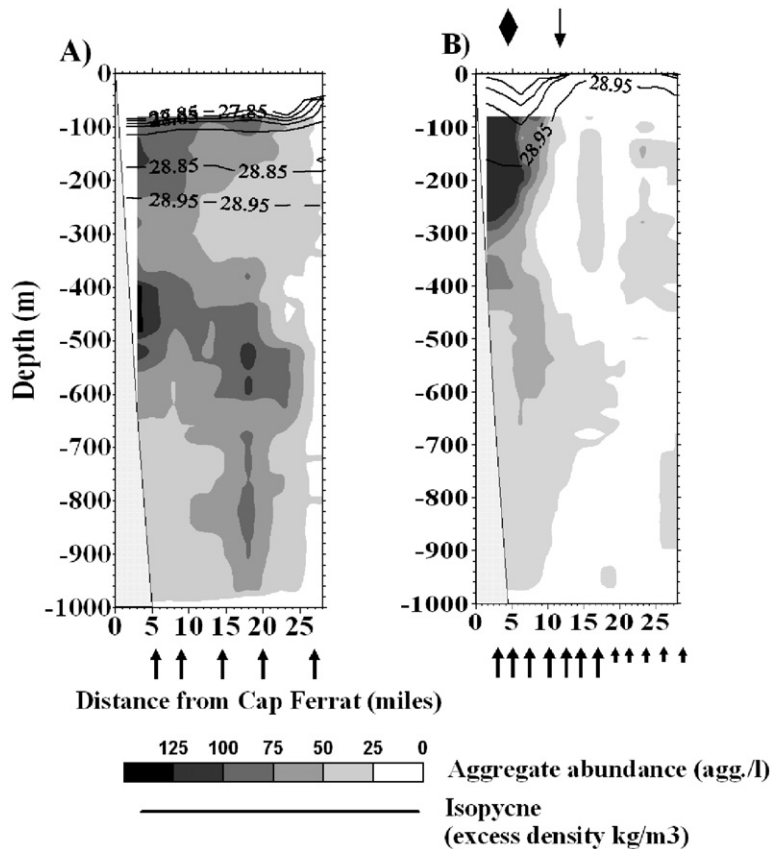


Fig. 9. Aggregate abundances along the transect, on (A) 9 November 1993 and (B) 8 March 1994. The arrows identify the stations (smaller arrows in B indicate the station sampled on the second day). Sampling was done over 1 day in November 1993, and 2 days in March 1994. The symbols ◆ and ↓ identify the two edges of the frontal zone in March 1994.

(out of 25), and significantly lower in 11 cases (out of 25); in one case out of 25 (i.e. October 1994), the frequency distributions were similar. The list of transects having higher ESD in the FZ compared to the PZ is given in Table 2. In contrast, the mean size was significantly higher in the FZ than in the CZ in 21 cases (out of 25).

## 5. Discussion

### 5.1. Influence of the frontal zone on the spatial distributions of SALs and IALs

Figs. 5 and 6 show that SALs and IALs are constant features along the slope. They are characterized by large spatial and temporal variability at the monthly scale, suggesting intermittent dynamics. The time series of aggregate concentrations at 5.5 miles offshore were not correlated to river runoff (Spearman's rank correlation,  $n=31$ ,  $r_s=0.07$  and  $p>0.1$ ), suggesting that other processes such as re-suspension by internal waves (Monaco

et al., 1990), variability in deep currents (Crassous et al., 1991; de Madron et al., 1999b), and seasonal biological production (Stemmann et al., 2002) may have influenced aggregate dynamics. In the absence of data, we will not discuss in detail the origins of the SALs and IALs, but will instead concentrate on their spatial distributions across the frontal structure. Their offshore limits between 15 to 20 miles correspond usually to the position of the front.

The potential effect of the front on the extent of the SALs and IALs can be best seen on Fig. 9, which shows two extremes situations with the front located either close to the coast or far offshore. In November 1993, the low density of the central water (Fig. 9A) and the low horizontal density gradient suggest that the front was located farther from the shore than 28 miles. Such an offshore position is rare, but had been previously reported (November 1985, Sammari et al., 1995). The upper water salinity was abnormally low ( $<37.05$ ), reflecting freshwater input. Precipitation (recorded at

Nice airport) and river flows were high in October 1993. The frontal structure may have been pushed offshore as a consequence of the strong input of freshwater, as previously observed by Béthoux et al. (1988). The offshore displacement of the frontal system in November 1993 corresponds to the maximum extension of several SALs and IALs in the central water during our 4-year survey. The patchy distribution of IALs may have reflected the spatial and temporal heterogeneity of continental inputs and the high variability in hydrodynamic conditions. Contrary to the November 1993 situation, the FZ in March 1994 was located close the coast, as suggested by the sharp density gradient between 8.5 and 13 miles (Fig. 9B). The SAL was confined to the coastal area, and the isolines of aggregate concentrations were parallel to the isopycnals. This suggests that weak cross-front transport of aggregates occurred in the 0–200 m water layer. In contrast below 350 m, the IAL tended to expand farther offshore but did not exceed 10.5 miles.

These two situations show that the horizontal gradients of aggregate concentrations in the SAL followed those of seawater densities, suggesting that lateral export was a function of the aggregate excess density and the position of the front. The FZ along the Northern Mediterranean Current was shown to be a limit for the INL spreading in the CZ (Copin-Montegut, 1988; Durrieu de Madron et al., 1990; de Madron et al., 1999b), and to limit the offshore spread of coastal planktonic species and fish larvae to the open sea (Pedrotti and Fenaux, 1992; Sabates and Olivar, 1996). Our data suggest that the FZ also prevents the

offshore spreading of aggregates, probably because these were carried away by the circulation.

### 5.2. Aggregation in and below the frontal system

In 13 of the 25 transects, the FZ showed significantly larger ESD than the PZ, and in 21 cases the FZ showed significantly larger ESD than the CZ. Hence, slightly more than half of the sections had larger ESDs in the FZ compared to the PZ. It is possible that this frequency was under-estimated, because the statistical procedure is based only on physical properties (i.e. location of the FZ), while aggregation processes also involve marine production or continental inputs. The best period for aggregation is from September to April, when the mesoscale activity is high and when the source particles are abundant due to marine production (from March to May and from September to October) or continental inputs (in November and December). Hence, lower probability of aggregation in the FZ is expected during summer because the current is weak and continental inputs and marine production are low. As a result, all five transects performed in July and August showed no significant ESD increase in the FZ. If we excluded these situations from the analysis, then the frequency of cases in which larger aggregates were observed in the FZ compared to the PZ would increase from 13 out of 25 to 13 out of 20. Since particle aggregation occurs also in coastal or oceanic zones (Riebesell, 1991a; Stemmann et al., 2002), the maxima of aggregates ESD should not be restricted only to frontal

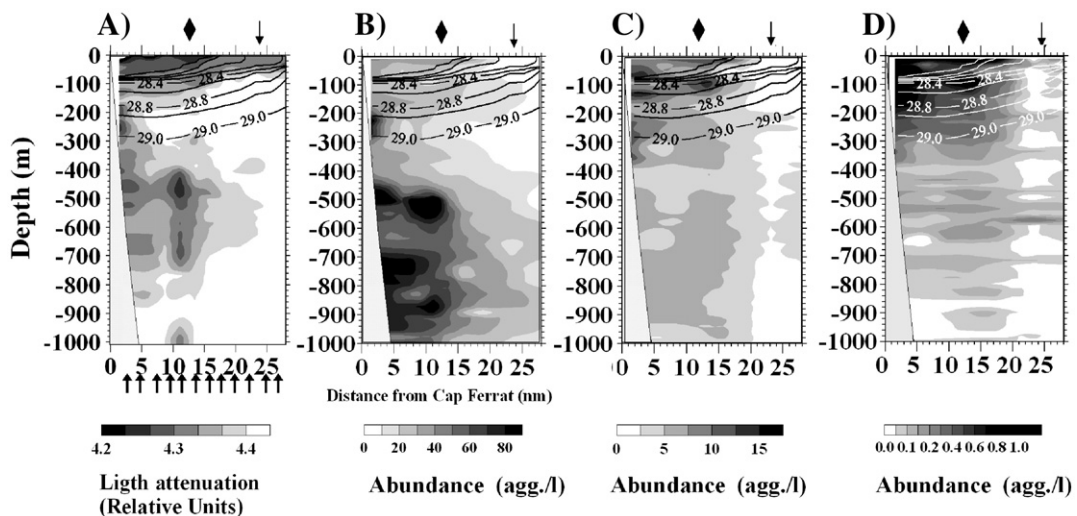


Fig. 10. Sections of spatial distribution of particles across the frontal system on the night of December 3 1994. (A) Suspended particulate matter load (light beam attenuation). Abundances of (B)  $0.15 < \text{aggregates} < 0.5$  mm, (C)  $0.5 < \text{aggregates} < 1$  mm and (D) aggregates  $> 1$  mm along the transect. The arrows indicate the positions of the stations. The symbols  $\blacklozenge$  and  $\blacktriangledown$  indicate the coastal and offshore limits of the front, respectively. The frontal zone is defined by these two boundaries.

systems. However, the relative high frequency of their observation in the FZ during our study suggests that specific processes enhance aggregation there.

In order to illustrate the spatial distribution of aggregates from the surface, Fig. 10 details the nighttime situations on 3 December 1994 (both night and day transects showed similar patterns in the 60–1000 m depth layer). Total aggregate abundances were higher in the PZ than in the CZ, and an IAL was observed along the continental slope between 400 and 950 m. The offshore extent of this layer was limited to 15.5 miles. The data obtained from the transmissometer attached to the UVP frame showed that the spatial pattern of submicron particles was similar to the one of aggregates <0.5 mm with a sharp decrease 13.5 miles offshore. Similar spatial pattern for INL and IAL has been observed in a previous study in the Gulf of Lions (de Madron et al., 1999b). The aggregate mean ESDs

were highest from 100 to 1000 m between 10.5 and 15.5 miles offshore in the FZ. The increase of aggregate mean ESD is due to the local increase in aggregates >1 mm (Fig. 10D) and the low concentration of aggregates <0.5 mm (Fig. 10B). The high concentration of aggregates >1 mm in the convergence zone of the frontal system and their decrease in concentration deeper suggests that they originate in the frontal water around 100 m, and that they were exported below the source of production.

Two aggregation mechanisms can explain the higher concentrations of aggregates >1 mm in the frontal system. First, small particles can coagulate efficiently in the frontal zone due to the higher turbulence level that enhances the cells encounter rates (Jackson, 1990). This process can occur at time scale relevant to the physical forcing (1–2 days), if the particle load is high enough and if the particles are sticky. These source particles

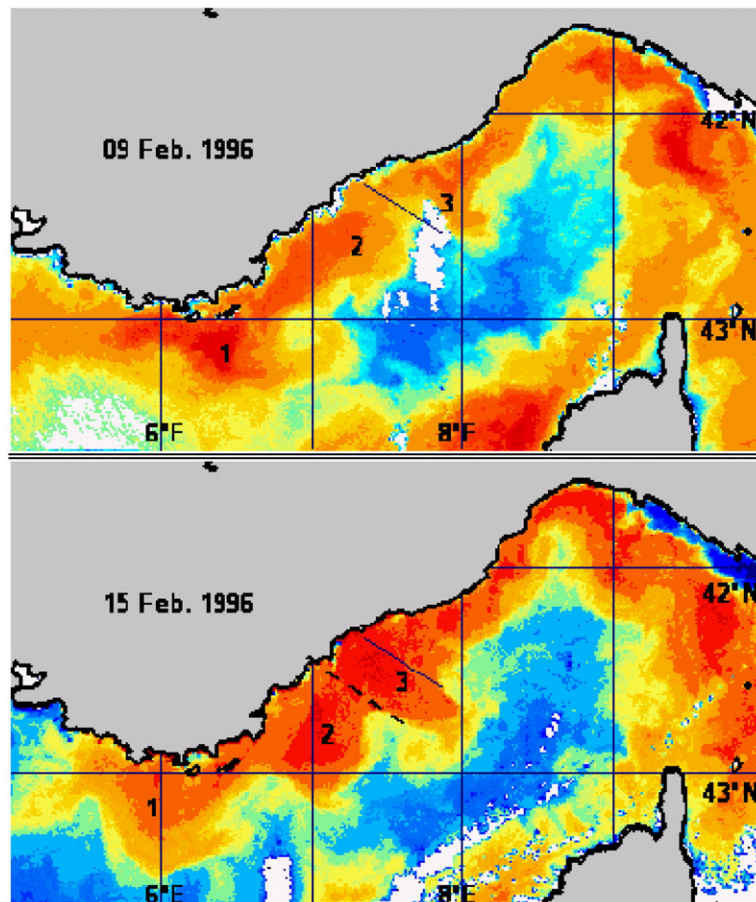


Fig. 11. NOAA/AVHRR Sea Surface Temperature (SST) image on the night of 8th to 9th of February 1996, and on 15th of February. The flow of AW appears as warmer temperatures (temp. increases from dark blue ( $\sim 14^{\circ}\text{C}$ ) to dark red ( $\sim 17^{\circ}\text{C}$ ); clouds are masked in white). The transect is defined by the dark line extending from the coast. The dotted line on the 15th of February indicates the virtual position, relative to the meander, of the transect on the 9th of February. There is a sharp meander just upstream the section on 9th of February, which has propagated southwest on the 15th of February. There are two other meanders (numbered from 1-older- to 3-younger-) propagating downstream.

could be produced locally from phytoplankton cells, or could be transported from the continental slope. The continental source may be important in spring and autumn when the river runoff is high. Second, an increase in zooplankton abundance and production of detritus can occur because frontal systems are zones of high trophic activity (Boucher et al., 1987; Legendre and Le Fèvre, 1989; Thibault et al., 1994). However, the concentration of zooplankton  $>1$  mm in the Mediterranean frontal area is too low to account for the observed number of aggregates. For example, the abundance of copepods  $>500$   $\mu\text{m}$  in size is less than  $3.5 \text{ ind. m}^{-3}$  in the top 200 m layer, compared to 1000 aggregates ( $>1$  mm)  $\text{m}^{-3}$  observed in the present study. Therefore, we suggest that most particles  $>1$  mm are aggregates produced in the frontal zone through biophysical processes (coagulation and biologically mediated aggregation) rather than living organisms.

Interestingly, the concentration of aggregates  $>1$  mm in the deep layer is high down to 800 m, suggesting efficient vertical export of the surface production. Such

efficient export is possible if the aggregates settle or are transported rapidly, or are produced while settling. The first mechanism is supported by the high settling speed of 1 mm aggregates, which ranges from  $50$  to  $300 \text{ m day}^{-1}$  (Aldredge and Gotschalk, 1988; Stemmann et al., 2002). In addition, high vertical velocity that has been observed in other highly hydrodynamic situation in the Western Mediterranean Sea could accelerate the downward transport of particles (van Haren and Millot, 2005). The second mechanism is supported by the observation that the INL and IAL which extend from the slope do not penetrate further offshore than the zone where large aggregate concentrations are high (Fig. 10). The horizontal decrease in concentration of small particles could be explained by scavenging. Indeed, the large fast settling particles, formed in the upper water column, would collide with the slow settling particles and build aggregates with them. This mechanism was proposed by Monaco et al. (1990) to explain the offshore limitation of continental inputs and the high flux of marine-snow type particles in sediment traps at the shelf break in the

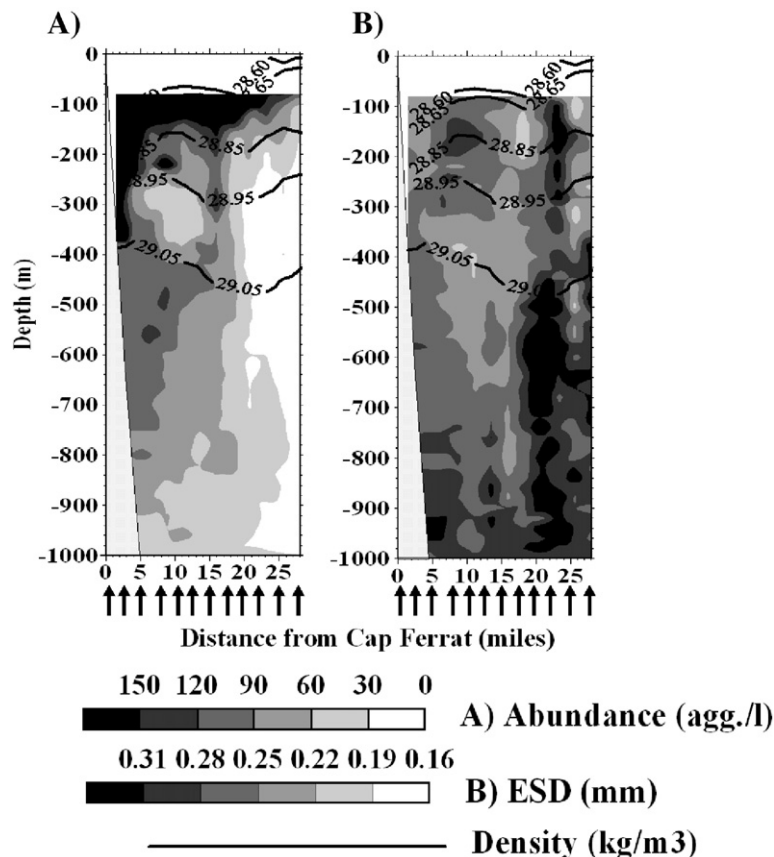


Fig. 12. (A) Aggregates abundance and (B) mean ESD along the same transect in February 1996. The arrows identify the stations which were all sampled at the same day.

Gulf of Lions. This mechanism could also explain why the IALs do not extend offshore beyond the frontal zone where the large aggregates are produced.

### 5.3. Effect of a meander on the spatial distribution of aggregates

The flow of the LC is not steady and exhibits meanders (Sammari et al., 1995) that can be used as a test for the conceptual model of cross-slope exchange of particles inferred from the above results. Previous work over the margin in the Gulf of Lions has shown that peaks of particle fluxes in sediment traps were more affected by intense cross-slope fluctuations of the current containing Atlantic Water than by large riverine or atmospheric inputs (de Madron et al., 1999b). In the present study, the isopycnals in February 1996 first showed a sharp upward slope, corresponding to the crossing of the part of the LC that flows along the slope ( $\sim 8$  miles wide), followed by a trough, corresponding to the crossing of the meander (Fig. 2B). The wave-like meandering structure of the current is clear from the sea surface temperature (Fig. 11). By 30th of January (data not shown) the meander had

built up and its western edge was upstream of the transect. By 9th of February, the meander was fully developed off the transect location, so that its edge (front) was located farther than 28 nautical miles offshore, and hence was not crossed. As the image on 9th of February (date of the transect) had a cloud right on the transect, we also show the cloud-free image on 15th of February, at which time the position of the transect had moved 22 km southwestwards, corresponding to a  $4 \text{ cm s}^{-1}$  of phase velocity of the meander (Fig. 11). Such velocity is close to the values from current meters and images in the same area in winter (Sammari et al., 1995). The structure may have reached a depth of 400 m, as suggested by drastic change in density at that depth (Fig. 12). The spatial distributions of both the total abundances and mean sizes of aggregates corresponded to the hydrological structure (Fig. 12). The mean sizes of aggregates were highest at the two shoreward edges of the density domes. Moreover, at 25.5 miles, the mean sizes were high down to 1000 m, suggesting that particles in the whole water column were affected by the frontal structure. The SAL was closely related to the density field, with the abundance maxima in the current. Thus, the February 1996 situation suggests that sub-

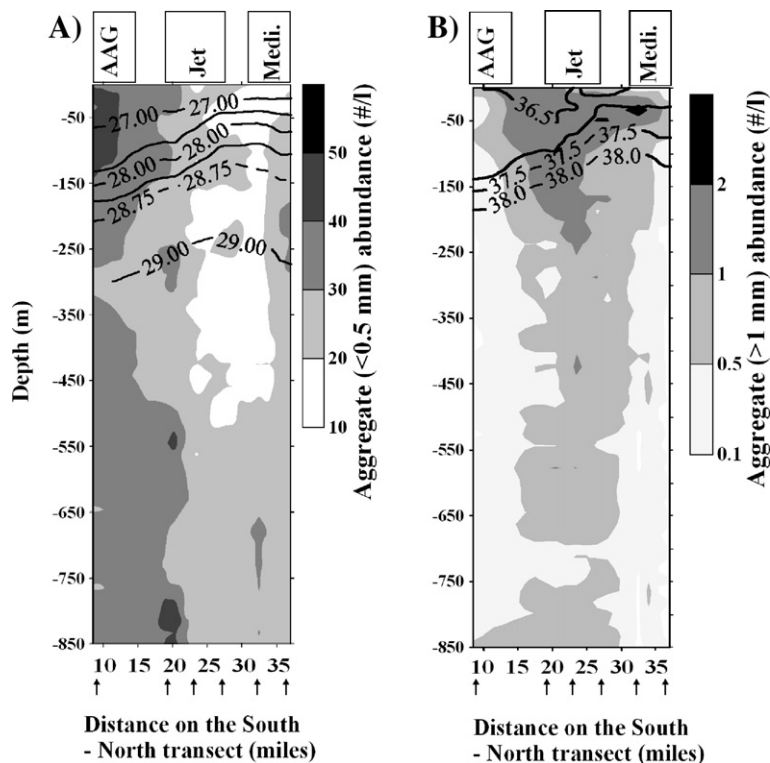


Fig. 13. (A) Spatial distribution of aggregates < 0.5 mm in ESD and isopycnals in the Almeria frontal system. (B) Spatial distribution of aggregates > 1 mm in ESD and isohalines (modified from Gorsky et al., 2002). The main flows of the Atlantic jet, the Atlantic Anticyclonic Gyre (AAG) and the Mediterranean Water are indicated. The horizontal distances are from the coast. The arrows identify the stations.

mesoscale processes occurring in the FZ may have had major effects on the dynamics of aggregates that confirm the aggregation pattern in highly dynamic current situation.

#### 5.4. Common features of the Ligurian and Almeria fronts, and potential effects along the AW flow in the Western Mediterranean

The ALMOFRONT I cruise took place in June 1991 in the Almeria frontal system in the Alboran Sea. Although this frontal structure differs slightly from the Ligurian frontal system (Prieur et al., 1993), the adjacent pelagic ecosystems are comparable (Zakardjian and Prieur, 1998). In this system, high concentrations of nutrients (Bianchi et al., 1994) and chlorophyll *a* (Fiala et al., 1994) were on the left-hand side of the jet (JET), while high particulate vertical fluxes (Peinert and Miquel, 1994) were recorded on the right-hand side in waters from the Atlantic Anticyclonic Gyre (AAG). By contrast, nutrient concentrations and vertical fluxes were low in the adjacent Mediterranean Water.

As in the Ligurian frontal system, the highest concentrations of aggregates larger than 1 mm were observed in the frontal area at the edge of the jet and the Mediterranean Water (Fig. 13). Their maximum abundances were found at 50 m depth in the divergence zone (corresponding to the peak of chlorophyll *a*), while deeper the high abundances were more in the convergence zone under the jet. The relatively high concentrations of aggregates > 1 mm are observed down to 850 m as in the Ligurian front. In contrast, the aggregates < 0.5 mm are found near the coast forming an SAL and an IAL extending from the coast, which suggests continental input. The offshore limit of this IAL corresponds to the site where large particles are abundant down to 1000 m depth. This leads to the conclusion that the laterally transported continental particles were scavenged by the large settling particles produced in the FZ. It follows that the general mechanism derived from the aggregate dynamics in the Ligurian frontal system may also apply to the Almeria frontal system.

In the Western Mediterranean Sea, the AW flows continuously following a general cyclonic path, and permanent fronts and eddies are ubiquitous features in that basin (Millot, 1999). The present study indicates that the spatio-temporal distribution of marine aggregates is profoundly affected by the general surface circulation along the path of the AW, and its effect on particle distribution is seen from surface down to at least 1000 m. In this continuous frontal structure, large aggregates are produced near the surface and sink. Thus, the frontal structure creates an “aggregate shower curtain”—a

curtain of settling particles. The offshore spread of the INLs may be stopped by this continuous biological barrier as proposed by Monaco et al. (1990) in the Gulf of Lion. Given the long path of the AW along the continental margins of the Western Mediterranean, the total vertical flux of particles over the whole basin may significantly reduce the seaward land–ocean transport of particles and increase vertical fluxes at fronts. The quantification of these interactions is not yet feasible due to lack of information on the spatial scales of the physical structures, and also on the properties of aggregates, i.e. mass and settling speed but is of considerable interest.

#### Acknowledgement

This research was undertaken in the framework of the MBP-Front and DYFAMED CNRS-INSU French JGOFS programs, and the French ZOOPEC program. We acknowledge the support of the European Commission’s Marine Science and Technology (MAST) Program under contract MAS3-CT96-0051. Contribution number MTP II-MATER/037. The NOAA/AVHRR Sea Surface Temperatures images were provided by SATMOS (<http://www.satmos.meteo.fr/>) INSU/Météo-France. We thank three anonymous reviewers for their contribution to improving the quality of the manuscript. We thank the captains and crews of the R/V Tethys, R.V. Pr. Georges Petit and R.V. Korotneff for their efficient assistance at sea.

#### References

- Albérola, C., Millot, C., Font, J., 1995. On the seasonal and mesoscale variabilities of the Northern Current during the PRIMO-0 experiment in the western Mediterranean Sea. *Oceanologica Acta* 18 (2), 163–192.
- Allredge, A.L., Gotschalk, C., 1988. In situ settling behavior of marine snow. *Limnology and Oceanography* 33 (3), 339–351.
- Allen, J.T., Brown, L., Sanders, R., Moore, C.M., Mustard, A., Fielding, S., Lucas, M., Rixen, M., Savidge, G., Henson, S., Mayor, D., 2005. Diatom carbon export enhanced by silicate upwelling in the northeast Atlantic. *Nature* 437 (7059), 728–732.
- Astraldi, M., Gasparini, G., 1992. The seasonal characteristics of the circulation in the North Mediterranean Basin and their relationship with the atmospheric-climatic conditions. *Journal of Geophysical Research* 92 (6), 9531–9540.
- Béthoux, J.-P., Prieur, L., 1983. Hydrologie et circulation en Méditerranée Nord-Occidentale. *Pétrole et Techniques* 299, 25–34.
- Béthoux, J.-P., Prieur, L., Nyffeler, F., 1982. The water circulation in the North Western Mediterranean Sea, its relation with wind and atmospheric pressure. *Hydrodynamics of semi enclosed seas*, pp. 129–142.
- Béthoux, J.-P., Prieur, L., Bong, J.H., 1988. Le courant Ligure au large de Nice. In: Nival, H.J.M.A.P. (Ed.), *Océanographie pélagique Méditerranéenne*, pp. 59–67.
- Bianchi, M., Morin, P., Lecorre, P., 1994. Nitrification rates, nitrite and nitrate distribution in the Almeria-Oran Frontal Systems (Eastern Alboran Sea). *Journal of Marine Systems* 5 (3–5), 327–342.

- Boucher, J., Ibanez, F., Prieur, L., 1987. Daily and seasonal variations in the spatial distribution of zooplankton populations in relation to the physical structure in the Ligurian front. *Journal of Marine Research* 45 (1), 133–173.
- Copin-Montegut, C., 1988. Major elements of suspended particulate matter from the western Mediterranean Sea. In: Minas, H.J., Nival, P. (Eds.), *Océanographie Pélagique Méditerranéenne*. Oceanologica Acta, Paris, pp. 95–102.
- Crassous, P., Khripounoff, A., La Rosa, J., Miquel, J.-C., 1991. Remises en suspension sédimentaires observées en Méditerranée par 2000 m de profondeur à l'aide de pièges à particules. *Oceanologica Acta* 14 (2), 115–121.
- Crépon, M., Boukthir, M., 1987. Effect of deep water formation on the circulation of the Ligurian Basin. *Annales Geophysicae* 5B, 43–48.
- Crépon, M., Wald, L., Monget, J.M., 1982. Low frequency waves in the Ligurian sea during December 1977. *Journal of Geophysical Research* 87, 595–600.
- de Madron, X.D., Castaing, P., Nyffeler, F., Courp, T., 1999a. Slope transport of suspended particulate matter on the Aquitanian margin of the Bay of Biscay. *Deep-Sea Research, Part II: Topical Studies in Oceanography* 46 (10), 2003–2027.
- de Madron, X.D., Radakovitch, O., Heussner, S., Loye-Pilot, M.D., Monaco, A., 1999b. Role of the climatological and current variability on shelf-slope exchanges of particulate matter: evidence from the Rhone continental margin (NW Mediterranean). *Deep-Sea Research, Part I: Oceanographic Research Papers* 46 (9), 1513–1538.
- Durrieu de Madron, X., Nyffeler, F., Godet, C.H., 1990. Hydrographic structure and nepheloid spatial distribution in the Gulf of Lions continental margin. *Continental Shelf Research* 10 (9–11), 915–929.
- Fiala, M., Sourmia, A., Claustre, H., Marty, J.C., Prieur, L., Vétion, G., 1994. Gradients of phytoplankton abundance, composition and photosynthetic pigments across the Almeria-Oran Front (SW Mediterranean-Sea). *Journal of Marine Systems* 5 (3–5), 223–233.
- Gardner, W.D., 1989. Baltimore canyon as a modern conduit of sediment to the deep sea. *Deep-Sea Research* 36, 323–358.
- Gardner, W.D., Walsh, I.D., 1990. Distribution of macroaggregates and fine-grained particles across a continental margin and their potential role in fluxes. *Deep-Sea Research* 37 (3), 401–411.
- Giordani, H., Prieur, L., Caniaux, G., 2006. Advanced insight into sources of vertical velocity in the ocean. *Ocean Dynamics* 56 (5), 1–12. doi:10.1007/s10236-005-0050-1.
- Goffart, A., Hecq, J.H., Prieur, L., 1995. Control of the phytoplankton of the Ligurian Basin by the Liguro-Provencal Front (Corsican Sector). *Oceanologica Acta* 18 (3), 329–342.
- Gorsky, G., Lins da Silva, N., Dallot, S., Laval, P., Braconnot, J.C., Prieur, L., 1991. Midwater tunicates: are they related to the permanent front of the Ligurian Sea (NW Mediterranean)? *Marine Ecology. Progress Series* 74 (2–3), 195–204.
- Gorsky, G., Aldorf, C., Kage, M., Picheral, M., Garcia, Y., Favole, J., 1992. Vertical distribution of suspended aggregates determined by a new underwater video profiler. *Annales de l'Institut Océanographique* 68 (1–2), 275–280.
- Gorsky, G., Prieur, L., Taupier-Letage, I., Stemann, L., Picheral, M., 2002. Large particulate matter in the Western Mediterranean I. LPM distribution related to mesoscale hydrodynamics. *Journal of Marine Systems* 33, 289–311.
- Guidi, L., Stemann, L., Legendre, L., Picheral, M., Prieur, L., Gorsky, G., 2007. Vertical distribution of aggregates (>110 µm) and mesoscale activity in the Northeastern Atlantic: effects on the deep vertical export of surface carbon. *Limnology and Oceanography* 52 (1), 7–18.
- Heussner, S., de Madron, X.D., Radakovitch, O., Beaufort, L., Biscaye, P.E., Carbonne, J., Delsaut, N., Etcheber, H., Monaco, A., 1999. Spatial and temporal patterns of downward particle fluxes on the continental slope of the Bay of Biscay (northeastern Atlantic). *Deep-Sea Research, Part II. Topical Studies in Oceanography* 46 (10), 2101–2146.
- Jackson, G.A., 1990. A model for the formation of marine algal flocs by physical coagulation processes. *Deep-Sea Research* 37, 1197–1211.
- Legendre, L., Le Fèvre, J., 1989. Hydrodynamical singularities as controls of recycled versus export production in oceans. In: Berger, W.H., Smetacek, V.S., Wefer, G. (Eds.), *Productivity of the Ocean: Present and Past*. John Wiley and Sons Limited, New-York.
- McCave, I.N., Hall, I.R., Antia, A.N., Chou, L., Dehairs, F., Lampitt, R.S., Thomsen, L., van Weering, T.C.E., Wollast, R., 2001. Distribution, composition and flux of particulate material over the European margin at 47 degrees–50 degrees N. *Deep-Sea Research, Part 2: Topical Studies in Oceanography* 48 (14–15), 3107–3139.
- Millot, C., 1999. Circulation in the Western Mediterranean Sea [Review]. *Journal of Marine Systems* 20 (1–4), 423–442.
- Monaco, A., Courp, T., Heussner, S., Carbonne, J., Fowler, S.W., Deniaux, B., 1990. Seasonality and composition of particulate fluxes during ECOMARGE-1, western Gulf of Lions. *Continental Shelf Research* 10 (9–11), 959–987.
- Pedrotti, M.L., Fenaux, L., 1992. Dispersal of echinoderm larvae in a geographical area marked by upwelling (Ligurian Sea, NW Mediterranean). *Marine Ecology. Progress Series* 86, 217–227.
- Peinert, R., Miquel, J.-C., 1994. The significance of frontal processes for vertical particle fluxes: a case study in the Alboran Sea (SW Mediterranean Sea). *Journal of Marine Systems* 5 (3–5), 377–389.
- Prieur, L., Bethoux, J.P., Albuissou, M., Wald, L., Monget, J.M., 1981. A comparison between infrared satellite images and sea truth measurements. *Oceanography from Space*. Plenum Press. 159–167 pp.
- Prieur, L., Bethoux, J.P., Bong, J.H., Tailliez, D., 1983. Particularités hydrologiques et formation d'eau profonde dans le bassin Liguro-Provencal en 1981–1982. *Rapport de la Commission Internationale de la Mer Méditerranée* 28 (2), 51–53.
- Prieur, L., Copin-Montegut, C., Claustre, H., 1993. Biophysical aspects of “ALMOFRONT-1”, an intensive study of a geostrophic frontal jet. *Annales de l'Institut Océanographique* 69 (1), 71–86.
- Riebesell, U., 1991a. Particle aggregation during a diatom bloom. I. Physical aspects. *Marine Ecology. Progress Series* 69, 273–280.
- Sabates, A., Olivar, M.P., 1996. Variation of larval fish distributions associated with variability in the location of a shelf-slope front. *Marine Ecology. Progress Series* 135 (1–3), 11–20.
- Sammari, C., Millot, C., Prieur, L., 1995. Aspects of the seasonal and mesoscale variabilities of the Northern Current in the western Mediterranean Sea inferred from the PROLIG-2 and PROS-6 experiments. *Deep-Sea Research* 42 (6), 893–917.
- Sourmia, A., Brylinski, J.-M., Dallot, S., Le Corre, P., Leveau, M., Prieur, L., Froget, C., 1990. Fronts hydrologiques au large des côtes françaises: Les sites-ateliers du programme Frontal. *Oceanologica Acta* 13 (4), 413–438.
- Stemann, L., Picheral, M., Gorsky, G., 2000. Diel variation in the vertical distribution of particulate matter (>0.15 mm) in the NW Mediterranean Sea investigated with the Underwater Video Profiler. *Deep-Sea Research, Part I: Oceanographic Research Papers* 47 (3), 505–531.
- Stemann, L., Gorsky, G., Marty, J.-C., Picheral, M., Miquel, J.-C., 2002. Four-year study of large-particle vertical distribution (0–1000 m) in the NW Mediterranean in relation to hydrology, phytoplankton, and

- vertical flux. *Deep-Sea Research, Part II: Topical Studies in Oceanography* 49 (11), 2143–2162.
- Taupier-Letage, I., Millot, C., 1986. General hydrodynamical features in the Ligurian Sea inferred from the DYOME experiment. *Oceanologica Acta* 2 (2), 119–131.
- Thibault, D., Gaudy, R., Lefevre, J., 1994. Zooplankton biomass, feeding and metabolism in a geostrophic frontal area (Almeria-Oran Front, Western Mediterranean)—significance to pelagic food webs. *Journal of Marine Systems* 5 (3–5), 297–311.
- van Haren, H., Millot, C., 2005. Gyroscopic waves in the Mediterranean Sea. *Geophysical Research Letters* 32 (24).
- Zakardjian, B., Prieur, L., 1998. Biological and chemical signs of upward motions in permanent geostrophic fronts of the Western Mediterranean. *Journal of Geophysical Research-Oceans* 103 (C12), 27849–27866.